

**Size distributions of
non-volatile particle
residuals and relation
to air mass origin**

C. Engler et al.

Size distributions of non-volatile particle residuals ($D_p < 800$ nm) at a rural site in Germany and relation to air mass origin

C. Engler¹, D. Rose¹, B. Wehner¹, A. Wiedensohler¹, E. Brüggemann¹,
T. Gnauk¹, G. Spindler¹, T. Tuch^{1,2}, and W. Birmili¹

¹Leibniz Institute for Tropospheric Research, Leipzig, Germany

²UFZ Center for Environmental Research, Department of Human Exposure Research and Epidemiology, Leipzig, Germany

Received: 9 March 2006 – Accepted: 22 May 2006 – Published: 27 June 2006

Correspondence to: W. Birmili (birmili@tropos.de)

Title Page

Abstract

Introduction

Conclusions

References

Tables

Figures

⏪

⏩

◀

▶

Back

Close

Full Screen / Esc

Printer-friendly Version

Interactive Discussion

Abstract

Atmospheric aerosol particle size distributions at a continental background site in Eastern Germany were examined for a one-year period. Particles were classified using a twin differential mobility particle sizer in a size range between 3 and 800 nm. As a novelty, every second measurement of this experiment involved the removal of volatile chemical compounds in a thermodenuder at 300°C. This concept allowed to quantify the number size distribution of non-volatile particle cores – primarily associated with elemental carbon, and to compare this to the original ambient size distribution. A general result was that practically every ambient particle in continental background air contained a non-volatile core. The volume fraction of non-volatile particulate matter (ambient $D_p < 800$ nm) varied between 10 and 30% and was largely consistent with the experimentally determined mass fraction of elemental carbon. The average size of the non-volatile particle cores was estimated as a function of original ambient size using a summation method, which showed that larger particles (>200 nm) contained more non-volatile compounds than smaller particles (<50 nm), thus indicating a significantly different chemical composition. Two alternative air mass classification schemes based on either, synoptic chart analysis (Berliner Wetterkarte) or back trajectories showed, that the volume and number fractions of non-volatile cores were less dependent on air mass than the absolute concentrations in the particle size distributions. In all air masses, the non-volatile size distributions showed a more and a less volatile (“soot”) mode, which is located in the size range of about 50 nm. During unstable conditions and in maritime air masses, smaller values were observed compared to continental or stable conditions. This reflects the significant emissions of non-volatile material over the continent and, depending on atmospheric stratification, increased concentrations at ground level.

ACPD

6, 5505–5542, 2006

Size distributions of non-volatile particle residuals and relation to air mass origin

C. Engler et al.

Title Page

Abstract

Introduction

Conclusions

References

Tables

Figures

⏪

⏩

◀

▶

Back

Close

Full Screen / Esc

Printer-friendly Version

Interactive Discussion

1 Introduction

Atmospheric aerosol particles have been recognized to play a key role in the balance of global climate, notably through their direct and indirect radiative effects (Haywood and Boucher, 2000). Anthropogenic aerosols shift the natural balance of radiation in the atmosphere, and rapidly changing and spatially diverse patterns of anthropogenic emissions make future projections of aerosol-driven climate effects a true challenge (Ramanathan et al., 2001). The aerosol particle size distribution is one of the key variables involved in the analysis of radiative aerosol effects, and consequently, numerous works have examined the spatio-temporal characteristics of particle size distributions under marine or arctic baseline conditions (e.g., Heintzenberg et al., 2004; Covert et al., 1996; Koponen et al., 2002), and in the continental atmospheres of Central Europe (Birmili et al., 2001), the Alps (Weingartner et al., 1999), Scandinavia (Mäkelä et al., 2000; Tunved et al., 2003), and Northern Italy (Rodríguez et al., 2005) with respect to the distribution of anthropogenic sources.

Particular efforts have been directed towards studying the relevance of atmospheric carbonaceous aerosols (e.g., Krivácsy et al., 2001). Black carbon is a strong absorber of visible light, whose radiative effect in mixed-phase particles and during cloud activation are uncertain to predict (Ackerman and Toon, 1981; Heintzenberg and Wendisch, 1996; Jacobson, 2001). Due to their insolubility, carbonaceous aerosols, particularly including elemental carbon, have also been associated with respiratory effects in animals and humans (Oberdörster, 2001; Donaldson et al., 2001).

Apart from volcanic activities and natural forest fires, black carbon stems overwhelmingly of anthropogenic sources, such as industrial and domestic combustion, and vehicular traffic sources (Ogren and Charlson, 1983; Andreae and Merlet, 2001; Bond et al., 2004). Modelling the emission, dispersion, and removal of carbonaceous aerosol requires spatially resolved emission inventories, which are usually difficult to obtain.

Atmospheric measurements using cost-efficient techniques are therefore desirable to obtain information on the distribution, sources, and processes determining the life-

Size distributions of non-volatile particle residuals and relation to air mass origin

C. Engler et al.

Title Page

Abstract

Introduction

Conclusions

References

Tables

Figures

⏪

⏩

◀

▶

Back

Close

Full Screen / Esc

Printer-friendly Version

Interactive Discussion

time of carbonaceous aerosol components. A standard method to determine atmospheric black carbon concentrations is filter collection, and subsequent thermal treatment and detection of CO₂ in a EC/OC analyzer (Turpin et al., 2000). Photometric measurement techniques, such as the aethalometer, or the PSAP (Bond et al., 1999) have the advantage of higher time resolution, but are typically not designed to distinguish particles according to particle size.

An alternative method to investigate carbonaceous aerosols is volatility analysis. A basic experimental approach involves heating of sample aerosol, thereby causing volatile fractions of PM to evaporate, and subsequent removal of the evaporated material. Such devices have been known as “thermodenuders” (Burtcher et al., 2001), which allow to distinguish bulk portions of chemical species that are less or more volatile, respectively.

During this work, we have applied a combination of a twin differential mobility particle sizer (TDMPMS) and a thermodenuder (TD) to examine the change in particle size distribution due to the removal of volatile species. Tropospheric aerosol samples were thus analyzed for a period of 12 months, and distinguished according to air masses. The potential of our experimental methods to provide a surrogate measurement for the number concentration of primary anthropogenic particles is discussed.

2 Experimental

Atmospheric measurements of ambient and non-volatile particle size distributions were carried out over a period of 12 months between 1 July 2003 and 30 June 2004 at the atmospheric research station of the Leibniz Institute for Tropospheric Research Melpitz in Eastern Germany (87 m a.s.l., 51°32' N and 12°54' E). The station is surrounded by flat grass lands, agricultural pastures and woodlands within several tens of kilometers, and neither obstacles nor larger sources of pollution lie within the immediate vicinity of the station. The comparison of previous aerosol measurements at Melpitz with other European sites shows that Melpitz observations are within the concentration range of

Size distributions of non-volatile particle residuals and relation to air mass origin

C. Engler et al.

Title Page

Abstract

Introduction

Conclusions

References

Tables

Figures

⏪

⏩

◀

▶

Back

Close

Full Screen / Esc

Printer-friendly Version

Interactive Discussion

the more anthropogenically influenced background sites (van Dingenen et al., 2004; Putaud et al., 2004).

Particle number size distributions upstream and downstream a thermodenuder were measured using a flow-regulated twin differential mobility particle sizer (TDMPS) (Birmili et al., 1999). This instrument consists of two differential mobility particle analyzers (Vienna type), connected to a condensation particle counter (model 3010, TSI, St. Paul, Minnesota, U.S.), and an ultrafine condensation particle counter (model 3025, TSI), respectively, which together encompass a total particle size range between 3 to 800 nm. Sheath air was supplied at a humidity below 5%. The aerosol inlet was equipped with an Andersen PM₁₀ head.

For the volatilization of sample aerosol, a thermodenuder (TD) following the design of Wehner et al. (2002) was used. Briefly, this TD consists of a heating section to remove the volatile material at a temperature of 300°C, and a cooling section where the evaporated gas-phase compounds are absorbed by active carbon in order to avoid re-condensation on the particles.

A measurement cycle of the TD/TDMPS combination consisted of a size distribution scan upstream the TD, followed by a scan downstream the TD. A scan duration of 10 min allowed for a time resolution of 20 min for both the ambient-state and thermally conditioned distributions. On condition that the ambient aerosol population fluctuates only moderately with time, the quasi parallel measurements of ambient and non-volatile size distributions were compared against each other, as described in Sect. 3.3.

An aerosol conditioning device like the thermodenuder causes particle losses during transport, notably due to Brownian diffusion or thermophoresis. To account for these effects, the measured size distributions were corrected for size-resolved transmission factors that were determined in the laboratory using test aerosols for a range of particle sizes (3–50 nm).

Size distributions of non-volatile particle residuals and relation to air mass origin

C. Engler et al.

Title Page

Abstract

Introduction

Conclusions

References

Tables

Figures

⏪

⏩

◀

▶

Back

Close

Full Screen / Esc

Printer-friendly Version

Interactive Discussion

3 Methodology

Since this work relies on the relatively unexplored technique of particle volatilization in a thermodenuder, several aspects of non-volatile particulate matter, such as external particle mixture are now established.

5 3.1 State of mixture of non-volatile particulate matter

When measuring non-volatile size distributions, the question arises whether this non-volatile material originates from an entirely separate particle type (external mixture), or from chemically mixed particles (internal mixture). Tandem differential mobility analyzer (V-TDMA) measurements at Melpitz showed that non-volatile particulate matter in an aged continental aerosol occurred in the shape of both entirely non-volatile particles, and non-volatile particle cores of chemically mixed particles (Philippin et al., 2004; Rose et al., 2006). Figure 1 illustrates such decomposition of a monodisperse particle population into a “non-volatile”, and a “partially volatile” mode in the V-TDMA-system.

To establish a better understanding of the size distributions of non-volatile residues, V-TDMA data from Rose et al. (2006) were revisited and combined with concurrent TD-TDMPS measurements from this work. While the TD-TDMPS measured complete size distributions, the V-TDMA provided information on external particle mixture for a range of monodisperse particle sizes. In the V-TDMA, particles were heated to 300°C like in the TD-TDMPS.

The combination of TD-TDMPS and V-TDMA data involved a simulation of the non-volatile size distributions from both the ambient TDMPS size distribution (3–800 nm), and V-TDMA decomposition information for the monodisperse particle sizes 30, 50, 80, and 150 nm. V-TDMA decomposition spectra were first interpolated over the entire TDMPS size, and then used to map each size bins of the ambient TDMPS distribution onto a resulting size distribution corresponding to the state downstream of the thermodenuder.

A comparison of the simulated non-volatile size distribution and the experimentally

Size distributions of non-volatile particle residuals and relation to air mass origin

C. Engler et al.

Title Page

Abstract

Introduction

Conclusions

References

Tables

Figures

⏪

⏩

◀

▶

Back

Close

Full Screen / Esc

Printer-friendly Version

Interactive Discussion

determined TDMPs distribution downstream the thermodenuder can be seen in Fig. 2, and shows a very good agreement in particle number >20 nm, and in particle volume <200 nm. This indicates that V-TDMA and TD-TDMPs data are consistent, and exhaustive in describing the volatilization process of the measured size distributions in the range 20–200 nm. Divergences between simulation and measurement outside this size range are ascribed to the non-availability of V-TDMA information.

The knowledge of external particle mixture allows to determine which non-volatile particles measured in the TD-TDMPs derive from entirely non-volatile particles, and which from originally larger, internally mixed particles. Figure 3 shows how the simulated non-volatile number distribution can be decomposed into these two particle types. Interestingly, the non-volatile particles measured above a size of approximately 140 nm belong overwhelmingly to the type of entirely non-volatile particles, whereas below 140 nm, they are predominantly the non-volatile residues of originally larger particles. Also note that the distribution of entirely non-volatile particles has its maximum concentration at about 100 nm, which is similar to the emission profile of diesel soot (Harris and Maricq, 2001).

Associating entirely non-volatile particles with primary soot particles (cf., e.g., Philipin et al., 2004; Rose et al., 2006), and partially volatile particles with those that have undergone atmospheric processing, we summarize our results in the shape of the following paradigm for atmospheric non-volatile particle distributions:

1. Non-volatile particles larger than a certain size (~ 140 nm) belong mostly to the type of entirely non-volatile particles, which are associated with primary soot particles from combustion sources.
2. Non-volatile particles smaller than a certain size (~ 140 nm) are mostly residues of originally larger, and chemically mixed particles; these particles have undergone physical and chemical transformation in the atmosphere, such as coagulation and the heterogeneous addition of ionic and organic secondary aerosol.
3. Although the distribution of entirely non-volatile particles has its maximum con-

Size distributions of non-volatile particle residuals and relation to air mass origin

C. Engler et al.

Title Page

Abstract

Introduction

Conclusions

References

Tables

Figures

⏪

⏩

◀

▶

Back

Close

Full Screen / Esc

Printer-friendly Version

Interactive Discussion

centration at about 100 nm, these particles are still outnumbered at that size by a factor of approximately 2.5 by the residues of chemically mixed particles.

This paradigm is presumed to be valid for observations at a rural background site in an anthropogenically influenced troposphere, such as over Central Europe.

3.2 Relation between non-volatile particle volume and chemical particle composition

We now discuss the classes of chemical compounds that may be associated with the measured non-volatile size distributions. [Rose et al. \(2006\)](#) proposed primary sources of soot, such as diesel engine emissions as responsible for the type of entirely non-volatile particles over a range of atmospheric conditions.

Secondary particulate mass in the European rural troposphere, in contrast, is dominated by sulfate, nitrate, and secondary organic compounds ([Putaud et al., 2004](#)). From a compilation of known boiling points and experimentally determined volatilization temperatures in Table 1, it can be seen that the salts of ammonium are completely volatile at 300°C, whereas the salts of Na, K and Ca are non-volatile.

For organic compounds, the situation is more complicated since the myriad of individual organic species is difficult to measure, and knowledge on the volatility properties of atmospherically relevant species remains scattered. An agreed convention to separate “organic” and “elemental” carbon has been the thermal treatment of filter-based samples at 340°C over the duration of two hours ([Cachier et al., 1989](#); [Kuhlbusch et al., 1998](#)). While it may be safe to assume that airborne elemental carbon will be preserved during passage through our thermodenuder at 300°C, it is not evident which fractions of organic carbon will eventually be removed during the transit time of several seconds.

To scrutinize the connection between the non-volatile particulate fraction and classes of chemical compounds, impactor samples that were collected over 24 h each at Melnitz in July and August 2003 were analyzed with regard to chemical particle composition, with sampling being concurrent to the TD-TDMPS measurements. The impactor

Size distributions of non-volatile particle residuals and relation to air mass origin

C. Engler et al.

Title Page

Abstract

Introduction

Conclusions

References

Tables

Figures

⏪

⏩

◀

▶

Back

Close

Full Screen / Esc

Printer-friendly Version

Interactive Discussion

Size distributions of non-volatile particle residuals and relation to air mass origin

C. Engler et al.

Title Page

Abstract

Introduction

Conclusions

References

Tables

Figures

⏪

⏩

◀

▶

Back

Close

Full Screen / Esc

Printer-friendly Version

Interactive Discussion

stage used for a comparison with the TD-TDMPS encompasses the accumulation mode with aerodynamic particle sizes between 140 and 420 nm. Ion-chromatography served to determine the mass concentration of Cl^- , NO_3^- , SO_4^{2-} , Ca^{2+} , K^+ , Mg^{2+} , Na^+ , and NH_4^+ , whereas a thermographic carbon analysis was applied to determine the mass concentrations of organic and elemental carbon, respectively. Briefly, organic carbon (OC) was volatilized at 650°C under pure nitrogen, and subsequently oxidized catalytically at 850°C. Elemental carbon was defined as the remaining matter detected from complete combustion at 650°C under pure oxygen. More details of the analytical techniques can be found elsewhere (Plewka et al., 2004).

In a first calculation, the mass fractions of the salts of ammonium on the one hand, and Na, K, Ca, and Mg on the other hand were determined by distributing the pool of anions towards the cations according to their ion charge. Then, the chemical mass fractions were converted into volumetric mass fractions using bulk assumptions on the density of the different classes of compounds. Finally, the total non-volatile mass fraction was calculated by considering elemental carbon, and the salts of Na, K, Ca, and Mg non-volatile, and compared to the non-volatile volume fraction determined from the TD-TDMPS.

For eight samples, the non-volatile volume fraction calculated from the TD-TDMPS measurements was between 0.04 and 0.12, whereas the volume fraction of non-volatile chemical compounds amounted to values between 0.03 and 0.2. Although being far from a precision closure experiment, these results suggest that the non-volatile fraction detected by the TD-TDMPS is accounted for by EC and the non-volatile inorganic salts of Na, K, Ca, and Mg. In the continental accumulation mode aerosol analyzed, EC and the mentioned inorganic salts were found to occur in a ratio of approximately 1:5 in non-volatile PM.

3.3 Summation method

In some of our former work, we developed a method to interpret dual size distribution data with regard to the changes occurring in a distribution after being conditioned, more

precisely, humidified (Birmili et al., 2004). This method is used here to relate ambient (unconditioned) and non-volatile (conditioned) particle size distributions. Briefly, the approach of the summation method is to associate particle number segments of equal concentration under both the conditioned and unconditioned particle size distributions.

5 Next, the ratio of the mean particle size of two corresponding particle number segments is calculated. This diameter ratio is interpreted as a particle “growth factor” in the case of humidification, or a particle “shrinking factor” in the case of particulate matter loss due to volatilization. The output discussed in this work are continuous size-dependent functions of particle shrinking factor that relate the residual size of non-volatile particle
10 cores to the particles’ original ambient size.

It must be stated that the output of the method can only be interpreted usefully, provided that the number of aerosol particles stays the same during the thermal conditioning step. (Otherwise, particle number segments in both distributions cannot be associated in an unambiguous way.) This prerequisite has therefore been carefully
15 examined, and indeed an average ratio of 1.16 ± 0.16 between the total number concentrations of non-volatile and ambient particles suggests that the output functions can be interpreted as average shrinking factors of particles of a certain original ambient size.

3.4 Air mass classification

20 Synoptic scale air masses are a useful concept to classify aerosol populations that are shaped by regional aerosol emissions, or during long-range transport. We classified aerosol populations at Melpitz using the daily weather chart “Berliner Wetterkarte” (Geb, 1981; Institut für Meteorologie, 2004), an analysis which takes into account back trajectories and the thermal properties of air masses. The Berliner Wetterkarte analysis
25 distinguishes different regions of climatic origin (A – arctic, P – subpolar, S – subtropic, T – tropic) and air mass character (m – maritime, x – mixed type, c – continental).

Figure 4 illustrates a selection of typical back trajectories arriving in Central Europe as well as transformations because of energetic conversions, like the warming of arctic

Size distributions of non-volatile particle residuals and relation to air mass origin

C. Engler et al.

Title Page

Abstract

Introduction

Conclusions

References

Tables

Figures

⏪

⏩

◀

▶

Back

Close

Full Screen / Esc

Printer-friendly Version

Interactive Discussion

Size distributions of non-volatile particle residuals and relation to air mass origin

C. Engler et al.

[Title Page](#)[Abstract](#)[Introduction](#)[Conclusions](#)[References](#)[Tables](#)[Figures](#)[⏪](#)[⏩](#)[◀](#)[▶](#)[Back](#)[Close](#)[Full Screen / Esc](#)[Printer-friendly Version](#)[Interactive Discussion](#)

(A) air into subpolar (P) and further into heated subpolar (Ps), or changes in character. The Berliner Wetterkarte classification addresses continental influences in that a conversion from the maritime (m) to the mixed (x) type usually occurs after a residence time of 24 h over the continent, and further conversion into the continental (c) type after 3–5 days.

For our analysis, the synoptic maps of the 850 hPa-level were analyzed and the air masses over the sampling site were determined. In addition, the exact times of frontal passages were identified using time series of locally measured meteorological data (temperature, humidity, rainfall) at Melpitz, which led to a distinction between subsequent air masses as fine as possible. Particle size distributions were subsequently averaged over the data sets corresponding to each air mass type.

3.5 Cluster analysis

Back trajectories have been recognized as a valuable tool to investigate the origin of air pollutants (Stohl, 1998). Consequently, back trajectory cluster analysis was applied in this work as an alternative method for an air mass classification of particle size distributions. Some major advantages of the cluster method are that it can be automated, and provides a higher degree of objectiveness than the synoptic classification described above.

We applied a k-means cluster algorithm, which was developed closely following the approach first reported by Dorling et al. (1992), and divided the entire dataset into a predetermined number of trajectory clusters. The groundwork of the cluster analysis were back trajectories calculated using the HYSPLIT4 (HYbrid Single-Particle Lagrangian Integrated Trajectory) model (Draxler and Hess, 2004).

In addition, vertical profiles of pseudopotential temperature calculated from regular radiosonde ascents at the Station Oppin, 50 km distant to Melpitz were used. Profiles of pseudopotential temperature have been incorporated in the variables to be clustered because vertical temperature profiles characterize the degree of vertical atmospheric stratification, which is of elementary importance to any surface measurement of atmo-

spheric constituents.

The following Euclidian distances were computed to express the spatial separation between two back trajectories i and j :

$$L_{ij} = \frac{1}{K} \sum_k \sqrt{\sum_{l=1}^3 a_l (x_{li} - x_{lj})^2}. \quad (1)$$

5 Here, K is the number of trajectory points. $K = 144$ was chosen to represent hourly back trajectory positions over 6 days. l is the dimension of the vector to be clustered, which includes the three variables of geographical latitude and longitude (both in Cartesian coordinates), and pseudopotential temperature. a_l are the weights required to create
10 three variables of equitable magnitude; a_1 , a_2 , and a_3 were chosen as 1.25 degree^{-1} , 0.8 degree^{-1} , and $10/1 \text{ K}^{-1}$. Notably, the choice of a_3 required prior test runs because temperature is a variable entirely dissimilar from geographical position.

In practice, the cluster algorithm was run for a range of cluster numbers between 3 and 14. Selecting a small number of clusters will generate larger, more representative
15 features of different aerosol types. The decision, how many clusters to use for the final discussion of the size distribution data reflected a compromise between simplicity of display (low n) and a more visible separation of the data clusters, and yielded the two options of $n=7$ (for $a_3=10$) and $n=11$ (for $a_3=1$).

4 Effects of air mass history

20 4.1 Berliner Wetterkarte air mass classification

First, the results obtained from a segregation of the 12-month size distribution data set into the various air mass types after the Berliner Wetterkarte are discussed. The

Size distributions of non-volatile particle residuals and relation to air mass origin

C. Engler et al.

Title Page

Abstract

Introduction

Conclusions

References

Tables

Figures

⏪

⏩

◀

▶

Back

Close

Full Screen / Esc

Printer-friendly Version

Interactive Discussion

frequency of occurrence of the air mass types can be seen in Table 2. A general result is that pronounced continental air (“c”) was only sampled on about 15% of the time.

Figure 5 shows the the typical (median) values of the ambient particle size distributions in each of the air masses. It can be noted that the overall differences in size distributions between the maritime (“m”) and the mixed (“x”) type air masses were relatively minor. A possible explanation is the location of the Melpitz sampling site in eastern Germany, i.e., surrounded by populated areas with anthropogenic aerosol sources. Clean maritime air, e.g., is required to cover a distance of at least 400 km over land before arriving at Melpitz, leaving enough time for the uptake of anthropogenic emissions. Maritime type air masses have, per definition, spent less than 24 h over land, but the continental influence is already visible in an increased total particle concentration.

In subpolar air masses, however, the difference between the maritime and mixed type on the one hand, and continental air on the other hand is significant (Fig. 5b). In maritime air, Aitken and accumulation mode were separated by a concentration minimum at most times. This minimum (sometimes also referred to as “Hoppel”-minimum) is thought to result from the activation of Aitken particles in non-precipitating clouds. In mixed-type and continental air masses, only one broad particle mode is usually observed with a concentration maximum between about 70 to 90 nm.

Figure 5f aggregates the air masses into only character categories, and again points out the different modal features of the size distributions in the air mass types “m”, “x”, and “c”. Another relevant observation is the gradual increase in accumulation mode concentration from maritime (3500 cm^{-3}) to continental (6200 cm^{-3}) air masses.

In contrast to the previous text, Fig. 6 concentrates on the non-volatile particle size distributions, i.e., those measured downstream the thermodenuder. Generally, the non-volatile size distributions show overall variations between different air masses of a magnitude similar to the unconditioned size distributions. Likewise, the highest total concentrations were observed in pronounced continental air masses.

The non-volatile size distributions are marked by one common feature: the original, nearly monomodal distributions (Fig. 5) tended to evolve into bimodal distributions after

Size distributions of non-volatile particle residuals and relation to air mass originC. Engler et al.

[Title Page](#)[Abstract](#)[Introduction](#)[Conclusions](#)[References](#)[Tables](#)[Figures](#)[⏪](#)[⏩](#)[◀](#)[▶](#)[Back](#)[Close](#)[Full Screen / Esc](#)[Printer-friendly Version](#)[Interactive Discussion](#)

thermal conditioning (Fig. 6). This bimodal shape is caused by the split-up of the ambient distribution maximum between 50 and 100 nm in the thermodenuder: Entirely non-volatile particles will remain at approximately the same size, whereas partially volatile particles will appear in the second non-volatile mode, around 10–20 nm (Fig. 6).

Entirely non-volatile particles were found to be scarce in the size range <30 nm (cf. Sect. 3.1). Therefore, the particle mode “B” in Fig. 6 (<30 nm) consists overwhelmingly of the non-volatile residues of originally larger particles, whereas the particle mode “A” (>30 nm) is composed of both entirely non-volatile particles and non-volatile residues of larger particles. It is therefore mode “A”, which is sensitive towards variations in the concentration of entirely non-volatile particles, and it is this mode which we associate with primary emissions from combustion, such as soot, in a rural aerosol.

The typical modal diameters of mode “A” are between 70 and 90 nm, and show a minor dependency of the air mass type only (Fig. 6). The latter observation confirms that the anthropogenic source contributions (associated with the non-volatile PM contribution) are similar in all wind directions from the Melpitz observation site. However, the concentration of mode “A” appears to be the most sensitive with regard to different air mass types. The highest concentration in mode “A” occurred in air masses “cPs”, which represent aged and dry continental air masses originating from Eastern Europe (cf. Fig. 4).

Mode “B”, the non-volatile particle mode <30 nm was, in contrast, less influenced by different air mass types. This suggests that these non-volatile cores of originally larger ambient particles are more homogeneously emitted, or generated in the wider area around the Melpitz site. The chemical composition of the non-volatile residues of these particles is unknown; while their evaporated material contained the inorganic substances with evaporation temperatures below 300°C (cf. Table 1), little is known about the thermal behavior of organic atmospheric particulate species. Wehner et al. (2005) previously analyzed particle formation events at Melpitz and found that particles <30 nm that were newly formed from gaseous species always had a non-volatile core at 300°C. A hypothesis raised in Wehner et al. (2005) was that organic aerosol species

Size distributions of non-volatile particle residuals and relation to air mass origin

C. Engler et al.

Title Page

Abstract

Introduction

Conclusions

References

Tables

Figures

⏪

⏩

◀

▶

Back

Close

Full Screen / Esc

Printer-friendly Version

Interactive Discussion

might polymerize within the particle phase, thus generating non-volatile particle material. Support to this hypothesis was recently obtained by laboratory experiments using atmospherically relevant organic species (Kalberer et al., 2004).

Figure 7 shows the diameter shrinking factors (SF) due to particle volatilization at 300°C. The shrinking factors SF represent an average ratio between particle diameters after and before conditioning in the thermodenuder. The larger the SF, the more non-volatile material was contained in the aerosol under investigation. In contrast to the size distributions, SF is an intensive variable that depends on the chemical composition of the particles, not on their absolute concentration. Since the calculation method described in Sect. 3.3 does not resolve external mixture, each value of SF corresponds to the average over the more and less volatile subfractions of particles at a given ambient size.

The principal observation for rural Melpitz aerosol was that accumulation mode particles contained more non-volatile material (SF=0.55 at 400 nm) than Aitken and nucleation mode particles (SF=0.37 at 30 nm). The two examples correspond to non-volatile volumetric fractions of 17 and 5%, respectively. This trend is systematic through all observations, and is interpreted as increasing fractions of elemental carbon, as well as crustal material with increasing particle size.

The air mass-related differences demonstrate an increased amount of non-volatile material especially in continental (“c”) air. The feature is best seen for particles >100 nm in the air mass type “cPs” in Fig. 7c, and reflects an enrichment of the chemical compounds associated with non-volatile PM, such as elemental carbon (see Sect. 3.2). Below 70 nm, only minor differences in SF were found for different air mass types; this implies that nucleation mode and young Aitken particles – which are typically only a few days old, tend to follow a more uniform spatial distribution regarding chemical composition than accumulation mode particles.

It is interesting to note that in maritime air masses, the functions of SF is not monotonous with particle size, but often have a minor maximum around 100 nm and a minor minimum at diameters above (Fig. 7). This points towards a size-segregated

Size distributions of non-volatile particle residuals and relation to air mass origin

C. Engler et al.

Title Page

Abstract

Introduction

Conclusions

References

Tables

Figures

⏪

⏩

◀

▶

Back

Close

Full Screen / Esc

Printer-friendly Version

Interactive Discussion

chemical composition, with a maximum amount of volatile material in particles of the size range 150–200 nm. The relative fraction of volatile material, such as ammonium sulfate and nitrate is expected to be especially large in particles that were activated the first time in a non-precipitating cloud (Hoppel et al., 1994; Birmili et al., 1999), and it is exactly the corresponding particle size range where we see the minor minimum in SF. In conclusion, our size segregated SF data are consistent with the picture of secondary aerosol formation in non-precipitating clouds, a process that is more likely to occur in the humid air masses belonging to the characters “m” and “x” than to “c”.

The state of external mixture of rural aerosol particles at Melpitz has been shown to be roughly bimodal in Sect. 3.1. Moreover, a relatively fixed diameter ratio could be seen between the sub-populations of non-volatile and more volatile particles after thermo-conditioning. We made use of this knowledge to retrieve the relative number fraction of these two populations in 150 nm particles from the 12-month dual size distribution data. The corresponding calculation showed that on annual average ca. 17% of the 150 nm particles were entirely non-volatile, i.e., associated with externally mixed soot in air masses “c”, and 6.5% in air masses “m”.

4.2 Cluster analysis

As an alternative to the Berliner Wetterkarte air mass analysis, a cluster analysis based on back trajectories and temperature profiles was performed for the entire dataset. In this section, the corresponding results are presented for the cluster numbers $n=7$, and $n=11$ and compared to the former analysis.

Figure 8 and Table 3 give an overview over the particle size distribution, back trajectories, trace gas concentration, and meteorological parameters that are representative for each of the clusters of the analysis $n=7$. Generally, the largest differences between different trajectory clusters could be seen in the size range >70 nm of ambient particles (Fig. 8d), i.e., the accumulation mode range. The highest concentrations occurred in cluster No. 5, which corresponds largely to the air mass type “cPs” reported before in the Berliner Wetterkarte analysis. The lowest concentration occurred in cluster No. 2,

Size distributions of non-volatile particle residuals and relation to air mass origin

C. Engler et al.

Title Page

Abstract

Introduction

Conclusions

References

Tables

Figures

⏪

⏩

◀

▶

Back

Close

Full Screen / Esc

Printer-friendly Version

Interactive Discussion

which corresponds to a fast moving, maritime air mass. In cluster No. 2, the average size distribution is evidently bimodal, showing the accumulation mode ($D_p \sim 200$ nm) as a shoulder to the Aitken mode ($D_p \sim 40$ nm). The diameter shrinking factor for cluster No. 2 shows a minimum between 150 and 200 nm, which indicates a high fraction of volatile compounds in the accumulation mode (see Fig. 8d), probably caused by liquid phase formation in non-precipitating clouds (cf. discussion above).

An important factor determining the observed accumulation mode concentrations is vertical atmospheric stability: Fig. 8b displays the average vertical profiles of virtual potential temperature for each cluster, obtained from radiosonde ascents. According to the figure, the atmosphere was vertically most stable in cluster No. 4 and most unstable in cluster No. 1. The three clusters with the highest atmospheric stability (4, 3, 5) were also associated with the highest accumulation mode concentrations. Conversely, the clusters with the highest instability (1, 2, 6) were associated with the lowest accumulation mode concentrations. A key result in this context is also the increased fraction of non-volatile chemical compounds ($SF=0.50$) under stable atmospheric conditions (Fig. 8f). The explanation for both increased particle numbers and SF is that under inhibited vertical mixing, anthropogenic emissions from the ground remain trapped in a shallow ground layer, and cannot be removed vertically. These findings emphasize that stable atmospheric stratification is the most important meteorological condition to cause high aerosol concentrations in the ground layer, even in rural areas.

Differences between different air masses can also be seen for nucleation mode particles <30 nm: The highest number concentrations (median values) were related to cluster No. 1 (Fig. 8d). The periods of cluster No. 1 were accompanied by the the highest frequency of new particle formation events (Table 3). Cluster No. 1 is representative for very unstable air, originating from the North Sea, and low levels of pollutants like NO_x (Table 3). In this weather, the sky is usually clear which leads to the likely photochemical production of aerosol precursors. The meteorological situation corresponding to cluster No. 1 appears to be the most favorable for atmospheric new particle formation in Melpitz, and emphasizes the great degree of meteorological control on new parti-

Size distributions of non-volatile particle residuals and relation to air mass origin

C. Engler et al.

Title Page

Abstract

Introduction

Conclusions

References

Tables

Figures

⏪

⏩

◀

▶

Back

Close

Full Screen / Esc

Printer-friendly Version

Interactive Discussion

cle formation events. Interestingly, these findings appear to have an equivalent in the Finnish boreal forest, where new particle formation was also observed most frequently with the outbreak of cold air masses (Nilsson et al., 2001).

It can be seen in Fig. 8e that the newly formed particles, which have an ambient size <30 nm, tend to have a non-volatile core <10 nm. As already mentioned, it is a current subject of speculation what the composition of these non-volatile remnants of newly formed particles is. Both sulfuric acid and sulfates are volatile at 300°C , so more research will be needed to explain particularly the role of organics during the growth of particles to final sizes between 20 and 50 nm.

An overview of the cluster analysis using $n=11$ clusters is now given in Fig. 9 and Table 4. These results are added because the representation using 11 trajectory clusters explained some features of the dataset more effectively. One advantage is the increased distinction between the resulting 11 mean trajectories (Fig. 9a) compared to the analysis for $n=7$.

A defined mode of less volatile particles ($D_p \sim 50$ nm) was not found in maritime but in mixed type air masses (No. 4, 8, 9 and 11) and was even more distinct in continental air (No. 5, 6 and 7). In this size range, cluster No. 10 (which is similar to the “xPs” type in the former section) showed the highest concentrations in both the ambient and the non-volatile size distribution, but no clear splitting up into two modes was observed.

Values of the diameter shrinking factor between 0.35 and 0.52 were observed in maritime, unstable air masses (No. 1, 2 and 3), while stable layered, continental air masses (No. 5, 6, 8) showed higher values between 0.4 and 0.57. One single exception was found in cluster No. 7, which is representing a continental air mass of medium stability. In this cluster, minimum values of the diameter shrinking factor (0.3 to 0.5) but high values of the SO_2 -concentration were found. This is why the aerosol particles of this cluster (especially in the size range <100 nm) are assumed to consist of a high sulfate fraction, which is volatile at 300°C .

As a general result it has to be pointed out, that the more an air mass is influenced by the continent and the more stable it is layered, the higher are the particle number con-

Size distributions of non-volatile particle residuals and relation to air mass origin

C. Engler et al.

Title Page

Abstract

Introduction

Conclusions

References

Tables

Figures

⏪

⏩

◀

▶

Back

Close

Full Screen / Esc

Printer-friendly Version

Interactive Discussion

centrations in the accumulation mode range and the fractions of non-volatile chemical compounds in the entire size range regarded.

5 Summary and conclusions

In this work, a new type of atmospheric data, a combined set of ambient and non-volatile particle number size distributions was explored with regard to the influence of synoptic scale air masses. Initial measurements by a Volatility-TDMA demonstrated that rural aerosol particles in the Melpitz region (diameter <200 nm) consist of at least two externally mixed volatility modes. The non-volatile particle mode was associated with an external mixture of mainly soot, whereas the more volatile mode is interpreted to represent all internally mixed particles containing inorganic ions, organic compounds, and a non-volatile residuum. Simulations and measurements of the size distributions of non-volatile particle cores using V-TDMA and TD-TDMPS data agreed well within the size range 20–200 nm, thereby encompassing most of the occurring total particle number.

Diameter shrinking factors were calculated that represent a diameter fraction of non-volatile material in an aerosol population. Typical values ranged between 0.37 and 0.55 for particles between 30 and 400 nm. The general increase of the diameter shrinking factor with increasing particle size is interpreted as a change of chemical particle composition with particle size, i.e., a relative enrichment of non-volatile compounds such as elemental carbon and the salts of alkali and earth alkali metals in larger particles.

A classification of the size distributions after synoptic scale air masses (“Berliner Wetterkarte”) and back trajectory cluster analysis showed that both the ambient-state and non-volatile particle size distributions at Melpitz varied significantly with air mass origin and character. Two distinct physical modes (i.e., Aitken and accumulation mode) were found in maritime air masses only, whereas continental aerosols showed overwhelmingly a single particle mode around 100 nm. The total number concentrations were higher by a typical factor of about two in continental air compared to maritime air

Size distributions of non-volatile particle residuals and relation to air mass origin

C. Engler et al.

Title Page

Abstract

Introduction

Conclusions

References

Tables

Figures

⏪

⏩

◀

▶

Back

Close

Full Screen / Esc

Printer-friendly Version

Interactive Discussion

(on average 5900 cm^{-3} and 3700 cm^{-3} , respectively).

The particle size range $>50 \text{ nm}$ showed its highest concentration in air masses of continental character. These eastern and continental European air masses involve long residence times (>4 days) of tropospheric air over densely populated land. Besides anthropogenic emissions, the reduced atmospheric humidity and, consequently, reduced wet deposition is an explanation for these accumulative effects. Notably, the highest diameter fraction of non-volatile particle material $>50 \text{ nm}$ correlated very consistently with the situations of highest atmospheric stability, and therefore confirm the accumulation of primary emissions in these air masses as a dominating effect controlling particle number concentration.

Using a combination of long-term TD-TDMPS size distributions and representative short-term V-TDMA information, we further estimated the number fraction of non-volatile (i.e., “soot”) particles of the total number concentration of 150 nm particles. These calculations yielded an average soot particle number fraction of 17% in continental, and 6.5% in maritime air masses over the 12-month observation period.

It is a noticeable result, that the highest particle concentrations in the size range $<50 \text{ nm}$ occurred mainly in air masses from the North Sea, and Scandinavia, all accompanied by relatively low levels of anthropogenic trace gases but also by unstable atmospheric stratification. The origin of these air masses does not correlate with the centers of anthropogenic pollution, so most of these particles are thought to be formed by secondary pathways. The noticeable correlation between secondary particles and unstable air indicates that the secondary particle formation process is controlled to a considerable degree by meteorological processes, rather than by peak values of potential gas phase precursors.

Acknowledgements. Parts of this work were funded by the FAT (Fördervereinigung Automobiltechnik).

We acknowledge funding through the German Federal Environment Agency (UBA) grant UFO-PLAN 203 432 57/05.

Back trajectories were calculated on the NOAA ARL READY Website using the HYSPLIT (HY-

Size distributions of non-volatile particle residuals and relation to air mass origin

C. Engler et al.

Title Page

Abstract

Introduction

Conclusions

References

Tables

Figures

⏪

⏩

◀

▶

Back

Close

Full Screen / Esc

Printer-friendly Version

Interactive Discussion

brid Single-Particle Lagrangian Integrated Trajectory) Model (Reference: Draxler, R. R. and Rolph, G. D., 2003, NOAA Air Resources Laboratory, Silver Spring, MD, USA).

References

- Ackerman, T. P. and Toon, O. B.: Absorption of visible radiation in atmosphere containing mixtures of absorbing and nonabsorbing particles, *Appl. Opt.*, 20, 3661–3668, 1981. [5507](#)
- Andreae, M. O. and Merlet, P.: Emission of trace gases and aerosols from biomass burning, *Global Biogeochem. Cycles*, 15, 955–966, 2001. [5507](#)
- Birmili, W., Stratmann, F., and Wiedensohler, A.: Design of a DMA-based size spectrometer for a large particle size range and stable operation, *J. Aerosol Sci.*, 30, 549–553, 1999. [5509](#), [5520](#)
- Birmili, W., Wiedensohler, A., Heintzenberg, J., and Lehmann, K.: Atmospheric particle number size distribution in central Europe: Statistical relations to air masses and meteorology, *J. Geophys. Res.*, 106, 32 005–32 018, 2001. [5507](#), [5537](#)
- Birmili, W., Nowak, A., Schwirn, K., Lehmann, K., Massling, A., and Wiedensohler, A.: A new method to accurately relate dry and humidified number size distributions of atmospheric aerosols, *J. Aerosol Sci., Abstracts of EAC, Budapest 2004*, 1, 15–16, 2004. [5514](#)
- Bond, T. C., Anderson, T. L., and Campbell, D.: Calibration and intercomparison of filter-based measurements of visible light absorption by aerosols, *Aerosol Sci. Technol.*, 30, 582–600, 1999. [5508](#)
- Bond, T. C., Streets, D. G., Yarber, K. F., Nelson, S. M., Woo, J.-H., and Klimont, Z.: A technology-based global inventory of black and organic carbon emissions from combustion, *J. Geophys. Res.*, 109, D14 203, doi:10.1029/2003JD003697, 2004. [5507](#)
- Burtscher, H., Baltensperger, U., Bukowiecki, N., Cohn, P., Hüglin, C., Mohr, M., Nyeki, S., Schmatloch, V., Streit, N., and Weingartner, E.: Separation of volatile and non-volatile aerosol fractions by thermodesorption: instrumental development and applications, *J. Aerosol Sci.*, 32, 427–442, 2001. [5508](#)
- Cachier, H., Bremond, M.-P., and Buat-Ménard, T.: Determination of atmospheric soot carbon with a simple thermal method, *Tellus*, 41B, 379–390, 1989. [5512](#)
- Covert, D. S., Wiedensohler, A., Aalto, P., Heintzenberg, J., McMurry, P. H., and Leck, C.:

ACPD

6, 5505–5542, 2006

Size distributions of non-volatile particle residuals and relation to air mass origin

C. Engler et al.

Title Page

Abstract

Introduction

Conclusions

References

Tables

Figures

◀

▶

◀

▶

Back

Close

Full Screen / Esc

Printer-friendly Version

Interactive Discussion

Size distributions of non-volatile particle residuals and relation to air mass origin

C. Engler et al.

[Title Page](#)[Abstract](#)[Introduction](#)[Conclusions](#)[References](#)[Tables](#)[Figures](#)[⏪](#)[⏩](#)[◀](#)[▶](#)[Back](#)[Close](#)[Full Screen / Esc](#)[Printer-friendly Version](#)[Interactive Discussion](#)

Aerosol number size distributions from 3 to 500 nm diameter in the arctic marine boundary layer during summer and autumn, *Tellus*, 48B, 197–212, 1996. [5507](#)

Donaldson, K., Stone, V., Clouter, A., Renwick, L., and MacNee, W.: Ultrafine particles, *J. Occup. Environ. Medicine*, 58, 194–199, 2001. [5507](#)

5 Dorling, S. R., Davies, T. D., and Pierce, C. E.: Cluster analysis: a technique for estimating the synoptic meteorological controls on air and precipitation chemistry method and applications, *Atmos. Environ.*, 26A, 2575–2581, 1992. [5515](#)

Draxler, R. R. and Hess, G. D.: Description of the HYSPLIT4 modeling system, NOAA Technical Memorandum, ERL, ARL–224, 2004. [5515](#)

10 Geb, M.: Klimatologische Grundlagen der Luftmassenbestimmung, (in German), Beilage zur Berliner Wetterkarte 50/81, Institut für Meteorologie, Freie Universität Berlin, 1981. [5514](#), [5537](#)

Harris, S. J. and Maricq, M. M.: Signature size distributions for diesel and gasoline engine exhaust particulate matter, *J. Aerosol Sci.*, 32, 749–764, 2001. [5511](#)

15 Haywood, J. and Boucher, O.: Estimates of the direct and indirect radiative forcing due to tropospheric aerosols: A review, *Rev. Geophys.*, 38, 513–543, 2000. [5507](#)

Heintzenberg, J. and Wendisch, M.: On the sensitivity of cloud albedo to the partitioning of particulate absorbers in cloudy air, *Contr. Atmos. Phys.*, 69, 491–499, 1996. [5507](#)

20 Heintzenberg, J., Birmili, W., Wiedensohler, A., Nowak, A., and Tuch, T.: Structure, variability and persistence of the submicrometer marine aerosol, *Tellus*, 56B, 357–367, 2004. [5507](#)

Hoppel, W. A., Frick, G. M., Fitzgerald, J. W., and Larson, R. E.: Marine boundary layer measurements of new particle formation and the effects nonprecipitating clouds have on aerosol size distribution, *J. Geophys. Res.*, 99, 14 443–14 459, 1994. [5520](#)

Institut für Meteorologie: Berliner Wetterkarte, Freie Universität Berlin, Germany, 2004. [5514](#), [5537](#)

25 Jacobson, M. Z.: Strong radiative heating due to the mixing state of black carbon in atmospheric aerosols, *Nature*, 409, 695–697, 2001. [5507](#)

Johnson, G. R., Ristovski, Z., and Morawska, L.: Method for measuring the hygroscopic behaviour of lower volatility fractions in an internally mixed aerosol, *J. Aerosol Sci.*, 35, 443–455, 2004. [5530](#)

30 Kalberer, M., Paulsen, D., Sax, M., Steinbacher, M., Dommen, J., Prevot, A. S. H., Fisseha, R., Weingartner, E., Franevich, V., Zenobi, R., and Baltensperger, U.: Identification of polymers as major components of atmospheric organic aerosols, *Science*, 303, 1659–1662, 2004.

- Koponen, I., Virkkula, A., Hillamo, R., Kerminen, V.-M., and Kulmala, M.: Number size distribution and concentrations of marine aerosols: Observations during a cruise between the English Channel and the coast of Antarctica, *J. Geophys. Res.*, 107, 4753, doi:10.1029/2002JD002533, 2002. [5507](#)
- Krivácsy, Z., Hoffer, A., Sárvári, Z., Temesi, D., Baltensperger, U., Nyeki, S., Weingartner, E., Kleefeld, S., and Jennings, S. G.: Role of organic and black carbon in the chemical composition of atmospheric aerosol at European background sites, *Atmos. Environ.*, 35, 6231–6244, 2001. [5507](#)
- Kuhlbusch, T. A. J., Hertlein, A.-M., and Schütz, L. W.: Sources, determination, monitoring, and transport of carbonaceous aerosols in Mainz, Germany, *Atmos. Environ.*, 32, 1097–1110, 1998. [5512](#)
- Lide, D. R. (Ed.): *CRC Handbook of chemistry and physics* (77th ed.), CRC Press, Boca Raton, Fl., 1996. [5530](#)
- Mäkelä, J. M., Koponen, I. K., Aalto, P., and Kulmala, M.: One-year data of submicron size modes of tropospheric background aerosol in southern Finland, *J. Aerosol Sci.*, 31, 595–611, 2000. [5507](#)
- Nilsson, E. D., Paatero, J., and Boy, M.: Effects of air masses and synoptic weather on aerosol formation in the continental boundary layer, *Tellus*, 53B, 462–478, 2001. [5522](#)
- Oberdörster, G.: Pulmonary effects of inhaled ultrafine particles, *International Archives of Occupational Environmental Health*, 74, 1–8, 2001. [5507](#)
- Ogren, J. A. and Charlson, R. J.: Elemental carbon in the atmosphere: cycle and lifetime, *Tellus*, 35B, 241–254, 1983. [5507](#)
- Philippin, S., Wiedensohler, A., and Stratmann, F.: Measurements of non-volatile fractions of pollution aerosols with an eight-tube volatility tandem differential mobility analyzer (VTDMA-8), *J. Aerosol Sci.*, 35, 185–203, 2004. [5510](#), [5511](#)
- Pinnick, R. G., Jennings, S. G., and Fernandez, G.: Volatility of aerosols in the arid southwestern United States, *J. Atmos. Sci.*, 44, 562–576, 1987. [5530](#)
- Plewka, A., Gnauk, T., Brüggemann, E., Neusüß, C., and Herrmann, H.: Size-resolved aerosol characterization for a polluted episode at the IfT research station Melpitz in Autumn 1997, *J. Atmos. Chem.*, 48, 131–156, 2004. [5513](#)
- Putaud, J.-P., Raes, F., van Dingenen, R., Brüggemann, E., Facchini, M.-C., Decesari, S., Fuzzi, S., Gehrig, R., Hüglin, C., Laj, P., Lorbeer, G., Maenhaut, W., Mihalopoulos, N., Müller,

Size distributions of non-volatile particle residuals and relation to air mass origin

C. Engler et al.

Title Page

Abstract

Introduction

Conclusions

References

Tables

Figures

⏪

⏩

◀

▶

Back

Close

Full Screen / Esc

Printer-friendly Version

Interactive Discussion

Size distributions of non-volatile particle residuals and relation to air mass origin

C. Engler et al.

Title Page

Abstract

Introduction

Conclusions

References

Tables

Figures

◀

▶

◀

▶

Back

Close

Full Screen / Esc

Printer-friendly Version

Interactive Discussion

K., Querol, X., Rodríguez, S., Schneider, J., Spindler, G., ten Brink, H., Tørseth, K., and Wiedensohler, A.: A European aerosol phenomenology – 2: Chemical characteristics of particulate matter at kerbsite, urban, rural and background sites in Europe, *Atmos. Environ.*, 38, 2579–2595, 2004. [5509](#), [5512](#)

5 Ramanathan, V., Crutzen, P. J., Kiehl, J. T., and Rosenfeld, D.: Aerosols, climate, and the hydrological cycle, *Science*, 294, 2119–2124, 2001. [5507](#)

Rodríguez, S., van Dingenen, R., Putaud, J.-P., Martins-Dos Santos, S., and Roselli, D.: Nucleation and growth of new particles in the rural atmosphere of Northern Italy – relationship to air quality monitoring, *Atmos. Environ.*, 39, 6734–6746, 2005. [5507](#)

10 Rose, D., Wehner, B., Ketzler, M., Engler, C., Voigtländer, J., Tuch, T., and Wiedensohler, A.: Atmospheric number size distributions of soot particles and estimation of emission factors, *Atmos. Chem. Phys.*, 6, 1021–1031, 2006. [5510](#), [5511](#), [5512](#)

Schmid, O., Eimer, B., Hagen, D. E., and Whitefield, P. D.: Investigation of volatility method for measuring aqueous sulfuric acid on mixed aerosols, *Aerosol Sci. Technol.*, 36, 877–889, 2002. [5530](#)

15 Stohl, A.: Computation, accuracy and applications of trajectories – a review and bibliography, *Atmos. Environ.*, 32, 947–966, 1998. [5515](#)

Tunved, P., Hansson, H.-C., Kulmala, M., Aalto, P., Viisanen, Y., Karlsson, H., Kristensson, A., Swietlicki, E., Dal Maso, M., Ström, J., and Komppula, M.: One year boundary layer aerosol size distribution data from five nordic background stations, *Atmos. Chem. Phys.*, 3, 2183–2205, 2003. [5507](#)

20 Turpin, B. J., Saxena, P., and Andrews, E.: Measuring and simulating particulate organics in the atmosphere: problems and prospects, *Atmos. Environ.*, 34, 2983–3013, 2000. [5508](#)

25 van Dingenen, R., Raes, F., Puteaud, J.-P., Baltensperger, U., Charron, A., Facchini, M.-C., Decassari, S., Fuzzi, S., Gehrig, R., Hansson, H.-C., Harrison, R. M., Hüglin, C., Jones, A. M., Laj, P., Lorbeer, G., Maenhaut, W., Palmgren, F., Querol, X., Rodríguez, S., Schneider, J., ten Brink, H., Tunved, P., Tørseth, K., Wehner, B., Weingartner, E., Wiedensohler, A., and Wählin, P.: A European aerosol phenomenology – 1: physical characteristics of particulate matter at kerbside, urban, rural and background sites in Europe, *Atmos. Environ.*, 38, 2561–2577, 2004. [5509](#)

30 Weast, R. C. and Astle, M. J. (Eds.): *CRC Handbook of chemistry and physics* (61st ed.), CRC Press, Boca Raton, FL, 1980. [5530](#)

Wehner, B., Philippin, S., and Wiedensohler, A.: Design and calibration of a thermodenuder

with an improved heating unit to measure the size-dependent volatile fraction of aerosol particles, *J. Aerosol Sci.*, 33, 1087–1093, 2002. [5509](#)

Wehner, B., Petäjä, T., Boy, M., Engler, C., Birmili, W., Tuch, T., Wiedensohler, A., and Kulmala, M.: The contribution of sulfuric acid and non-volatile compounds on the growth of freshly formed atmospheric aerosols, *Geophys. Res. Lett.*, 32, L17810, doi:10.1029/2005GL023827, 2005. [5518](#)

Weingartner, E., Nyeki, S., and Baltensperger, U.: Seasonal and diurnal variation of aerosol size distributions ($10 < D < 750$ nm) at a high-alpine site (Jungfraujoch 3580 m a.s.l.), *J. Geophys. Res.*, 104, 26 809–26 820, 1999. [5507](#)

ACPD

6, 5505–5542, 2006

Size distributions of non-volatile particle residuals and relation to air mass origin

C. Engler et al.

Title Page

Abstract

Introduction

Conclusions

References

Tables

Figures

⏪

⏩

◀

▶

Back

Close

Full Screen / Esc

Printer-friendly Version

Interactive Discussion

Size distributions of non-volatile particle residuals and relation to air mass origin

C. Engler et al.

Title Page

Abstract

Introduction

Conclusions

References

Tables

Figures

◀

▶

◀

▶

Back

Close

Full Screen / Esc

Printer-friendly Version

Interactive Discussion

Table 1. Boiling points (BP) and volatilization temperatures T_{vol} of various compounds in pure form.

| Species | name | BP [°C] | T_{vol} [°C] |
|---|--------------------|-------------------|-------------------------------------|
| NaCl | sodium chloride | 1465 ^a | >300 ^{b,c,d} |
| Na ₂ SO ₄ | sodium sulfate | >300 ^a | >300 ^b |
| NaHSO ₄ | sodium bisulfate | – | >300 ^b |
| NaNO ₃ | sodium nitrate | – | >300 ^b |
| (NH ₄) ₂ SO ₄ | ammonium sulfate | d | 200 ^b ,205 ^d |
| NH ₄ HSO ₄ | ammonium bisulfate | d | 200 ^b ,202 ^d |
| NH ₄ NO ₃ | ammonium nitrate | 210 ^e | 75 ^d |
| NH ₄ Cl | ammonium chloride | 338 ^a | 135 ^b |
| H ₂ SO ₄ | sulfuric acid | 337 ^a | 139 ^d , 125 ^c |
| CaSO ₄ | calcium sulfate | – | >300 ^b |
| Ca(NO ₃) ₂ | calcium nitrate | – | >300 ^b |
| CaCl | calcium chloride | 1935 ^a | >300 ^b |
| KNO ₃ | potassium nitrate | 400 ^a | – |

^aLide (1996)

^bPinnick et al. (1987)

^cSchmid et al. (2002)

^dJohnson et al. (2004)

^eWeast and Astle (1980)

d: decomposes before boiling

Size distributions of non-volatile particle residuals and relation to air mass origin

C. Engler et al.

Table 2. Frequency of occurrence (FO) of the different air mass types at Melpitz between July 2003 and June 2004.

| maritime (m) | | mixed type (x) | | continental (c) | |
|--------------|--------|----------------|--------|-----------------|--------|
| name | FO [%] | name | FO [%] | name | FO [%] |
| mA | 5.1 | xA | 1.9 | cA | 0.0 |
| mP | 26.8 | xP | 7.8 | cP | 2.9 |
| mPs | 7.5 | xPs | 14.0 | cPs | 5.4 |
| mSp | 4.4 | xSp | 8.5 | cSp | 2.4 |
| mS | 5.0 | xS | 4.5 | cS | 3.8 |
| total | 48.8 | total | 36.7 | total | 14.5 |

[Title Page](#)
[Abstract](#)
[Introduction](#)
[Conclusions](#)
[References](#)
[Tables](#)
[Figures](#)
[⏪](#)
[⏩](#)
[◀](#)
[▶](#)
[Back](#)
[Close](#)
[Full Screen / Esc](#)
[Printer-friendly Version](#)
[Interactive Discussion](#)

Size distributions of non-volatile particle residuals and relation to air mass origin

C. Engler et al.

Table 3. Back trajectory cluster analysis for 7 air mass types: General air mass properties, frequency of nucleation events, mean trace gas concentrations [$\mu\text{g}/\text{m}^3$], temperature (T) [$^{\circ}\text{C}$] and wind speed (WS) [m/s].

| Cluster # | Origin | Stratification | Trajectories | Nucleation days | NO | O ₃ | SO ₂ | NO _x | T | WS |
|-----------|--------------------|----------------|--------------|-----------------|-----|----------------|-----------------|-----------------|------|-----|
| 1 | North Sea | very unstable | 100 | 41 | 1.2 | 84.5 | 3.5 | 8.0 | 18.0 | 3.0 |
| 2 | Atlantic | unstable | 126 | 14 | 1.3 | 54.2 | 2.6 | 9.3 | 10.5 | 3.8 |
| 3 | Western Europe | stable | 85 | 1 | 3.3 | 26.4 | 3.7 | 22.4 | 7.5 | 1.7 |
| 4 | North Sea, Germany | very stable | 29 | 1 | 5.0 | 18.5 | 5.5 | 24.6 | 3.4 | 1.7 |
| 5 | Eastern Europe | stable | 35 | 6 | 1.9 | 35.6 | 6.0 | 16.6 | 4.2 | 1.8 |
| 6 | Baltic states | unstable | 61 | 7 | 1.9 | 50.7 | 3.7 | 13.0 | 6.4 | 1.8 |
| 7 | North Sea | neutral | 132 | 6 | 2.0 | 37.9 | 2.9 | 15.2 | 9.2 | 1.5 |

[Title Page](#)
[Abstract](#)
[Introduction](#)
[Conclusions](#)
[References](#)
[Tables](#)
[Figures](#)
[Back](#)
[Close](#)
[Full Screen / Esc](#)
[Printer-friendly Version](#)
[Interactive Discussion](#)

Size distributions of non-volatile particle residuals and relation to air mass origin

C. Engler et al.

Table 4. Back trajectory cluster analysis for 11 air mass types: General air mass properties, frequency of nucleation events, mean trace gas concentrations [$\mu\text{g}/\text{m}^3$], temperature (T) [$^{\circ}\text{C}$] and wind speed (WS) [m/s].

| Cluster # | Origin | Stratification | Trajectories | Nucleation days | NO | O ₃ | SO ₂ | NO _x | T | WS |
|-----------|--------------------------|----------------|--------------|-----------------|-----|----------------|-----------------|-----------------|------|-----|
| 1 | North Sea | unstable | 55 | 7 | 1.7 | 49.8 | 2.3 | 11.5 | 9.2 | 2.9 |
| 2 | Atlantic | unstable | 43 | 4 | 1.3 | 53.2 | 2.4 | 8.5 | 8.9 | 4.0 |
| 3 | Atlantic, Western Europe | unstable | 77 | 9 | 1.2 | 54.0 | 3.1 | 10.3 | 12.1 | 3.8 |
| 4 | Western Europe | neutral | 67 | – | 2.6 | 29.7 | 3.8 | 20.1 | 7.7 | 2.1 |
| 5 | Germany | very stable | 23 | 1 | 4.5 | 14.6 | 6.2 | 25.4 | 3.3 | 1.5 |
| 6 | Germany | neutral | 58 | 3 | 3.7 | 31.4 | 4.2 | 21.1 | 9.3 | 1.3 |
| 7 | Eastern Europe | neutral | 29 | 3 | 2.1 | 42.4 | 6.1 | 15.9 | 6.1 | 1.8 |
| 8 | Baltic states | neutral | 21 | 6 | 1.6 | 50.1 | 4.8 | 11.0 | 2.4 | 2.3 |
| 9 | Baltic Sea | very unstable | 59 | 16 | 1.7 | 66.5 | 3.1 | 10.9 | 11.9 | 1.8 |
| 10 | Scandinavia | neutral | 34 | 2 | 2.7 | 32.1 | 2.9 | 17.4 | 7.0 | 0.9 |
| 11 | North Sea, Germany | very unstable | 102 | 25 | 1.3 | 66.4 | 3.0 | 10.8 | 14.6 | 2.4 |

Title Page

Abstract

Introduction

Conclusions

References

Tables

Figures

⏪

⏩

◀

▶

Back

Close

Full Screen / Esc

Printer-friendly Version

Interactive Discussion

Size distributions of non-volatile particle residuals and relation to air mass origin

C. Engler et al.

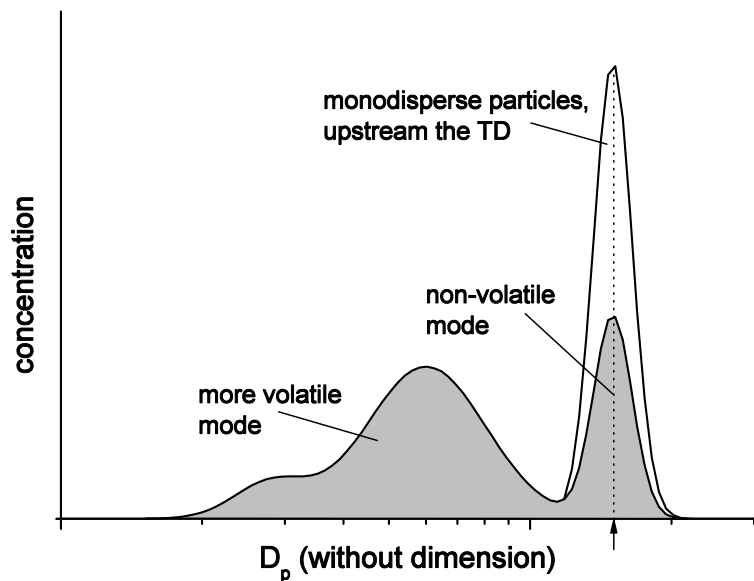


Fig. 1. Size distribution before (line) and after (grey area and bold line) thermal conditioning in the V-TDMA. The arrow shows the initial particle diameter (e.g., 30, 50, 80 or 150 nm).

Title Page

Abstract

Introduction

Conclusions

References

Tables

Figures

⏪

⏩

◀

▶

Back

Close

Full Screen / Esc

Printer-friendly Version

Interactive Discussion

Size distributions of non-volatile particle residuals and relation to air mass origin

C. Engler et al.

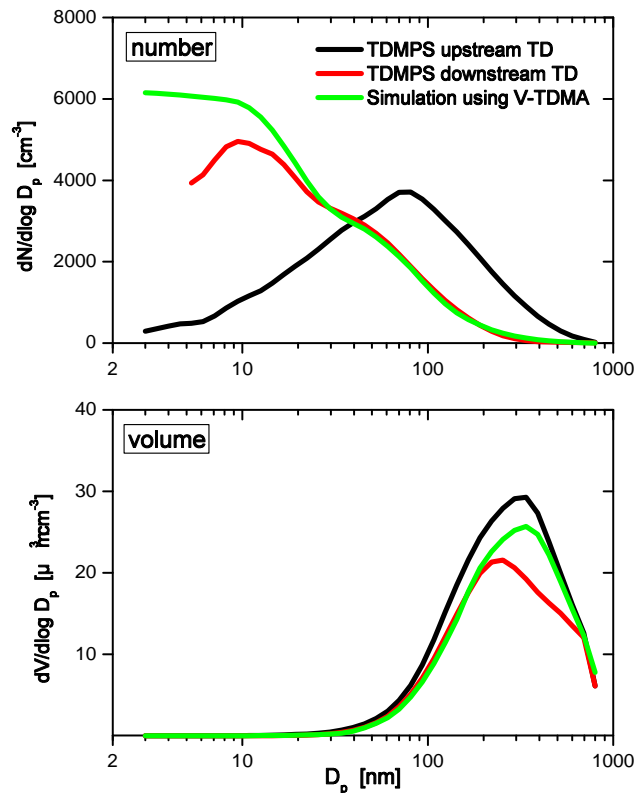


Fig. 2. Particle size distributions measured by the TDMPS upstream and downstream the thermodenuder **(a)**: number, **(b)**: volume. Green lines represent the distribution simulated from TDMPS (upstream) and V-TDMA external mixture information at sizes of 30, 50, 80, and 150 nm. The data refers to a 6 h measurement period between 06:00 and 18:00 h on 24 August 2003.

[Title Page](#)[Abstract](#)[Introduction](#)[Conclusions](#)[References](#)[Tables](#)[Figures](#)[◀](#)[▶](#)[◀](#)[▶](#)[Back](#)[Close](#)[Full Screen / Esc](#)[Printer-friendly Version](#)[Interactive Discussion](#)

Size distributions of non-volatile particle residuals and relation to air mass origin

C. Engler et al.

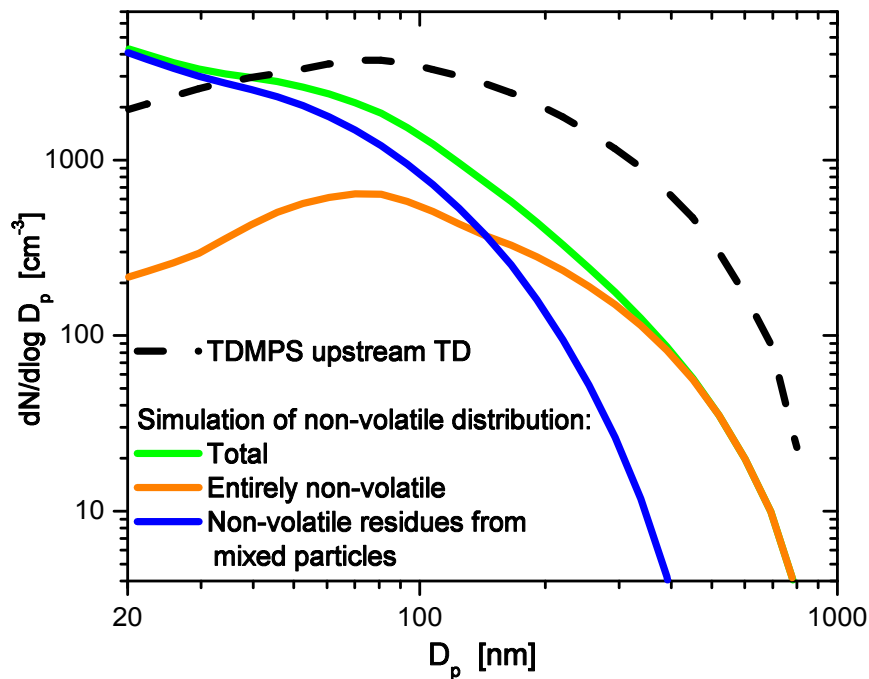


Fig. 3. Decomposing simulated non-volatile particle number distributions into externally mixed non-volatile particles (“primary soot”), and the non-volatile cores of internally mixed particles. The curves refer to the same data set as those in Fig. 2.

[Title Page](#)[Abstract](#)[Introduction](#)[Conclusions](#)[References](#)[Tables](#)[Figures](#)[◀](#)[▶](#)[◀](#)[▶](#)[Back](#)[Close](#)[Full Screen / Esc](#)[Printer-friendly Version](#)[Interactive Discussion](#)

Size distributions of non-volatile particle residuals and relation to air mass origin

C. Engler et al.

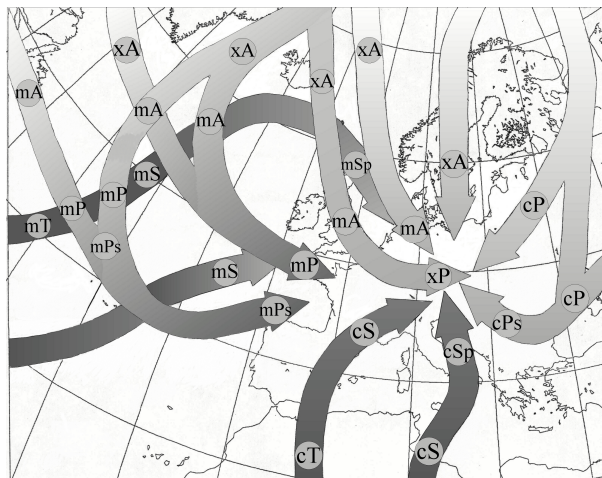


Fig. 4. Trajectories of air masses on their way to central Europe as well as transformations because of changes in heat content and character. After Geb (1981), supplement of Institut für Meteorologie (2004). From Birmili et al. (2001), Copyright [2001] American Geophysical Union. Reproduced by permission of American Geophysical Union.

Title Page

Abstract

Introduction

Conclusions

References

Tables

Figures

◀

▶

◀

▶

Back

Close

Full Screen / Esc

Printer-friendly Version

Interactive Discussion

Size distributions of non-volatile particle residuals and relation to air mass origin

C. Engler et al.

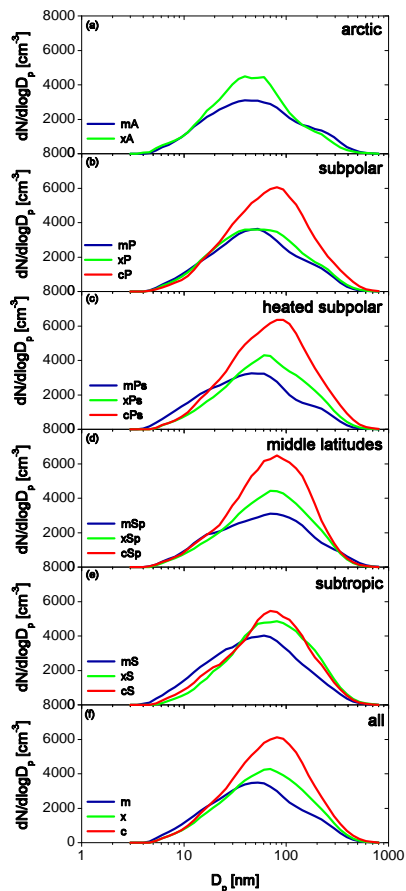


Fig. 5. Maritime (m), mixed type (x) and continental (c) character ambient particle size distributions (median values) for different air mass origin according to the air mass classification.

Title Page

Abstract

Introduction

Conclusions

References

Tables

Figures

◀

▶

◀

▶

Back

Close

Full Screen / Esc

Printer-friendly Version

Interactive Discussion

Size distributions of non-volatile particle residuals and relation to air mass origin

C. Engler et al.

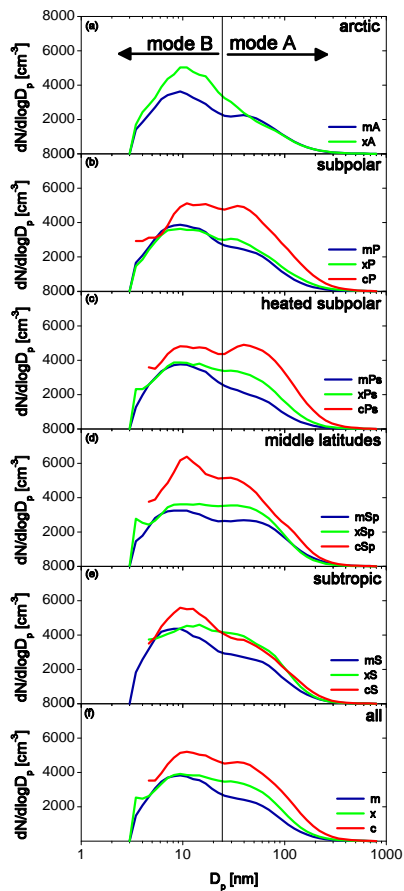


Fig. 6. Maritime (m), mixed type (x) and continental (c) character non-volatile particle size distributions (median values) for different air mass origin according to the air mass classification.

Title Page

Abstract

Introduction

Conclusions

References

Tables

Figures

◀

▶

◀

▶

Back

Close

Full Screen / Esc

Printer-friendly Version

Interactive Discussion

Size distributions of
non-volatile particle
residuals and relation
to air mass origin

C. Engler et al.

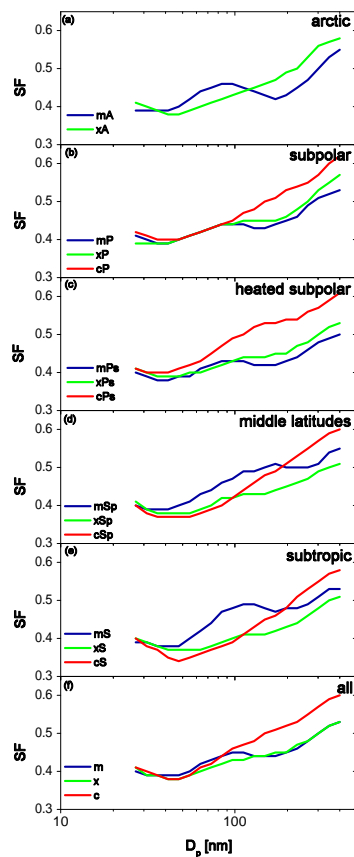


Fig. 7. Diameter shrinking factors (SF) as a function of ambient particle size due to volatilization at 300°C. Different curves correspond to SF in maritime (m), mixed type (x) and continental (c) air masses.

[Title Page](#)[Abstract](#)[Introduction](#)[Conclusions](#)[References](#)[Tables](#)[Figures](#)[◀](#)[▶](#)[◀](#)[▶](#)[Back](#)[Close](#)[Full Screen / Esc](#)[Printer-friendly Version](#)[Interactive Discussion](#)

Size distributions of non-volatile particle residuals and relation to air mass origin

C. Engler et al.

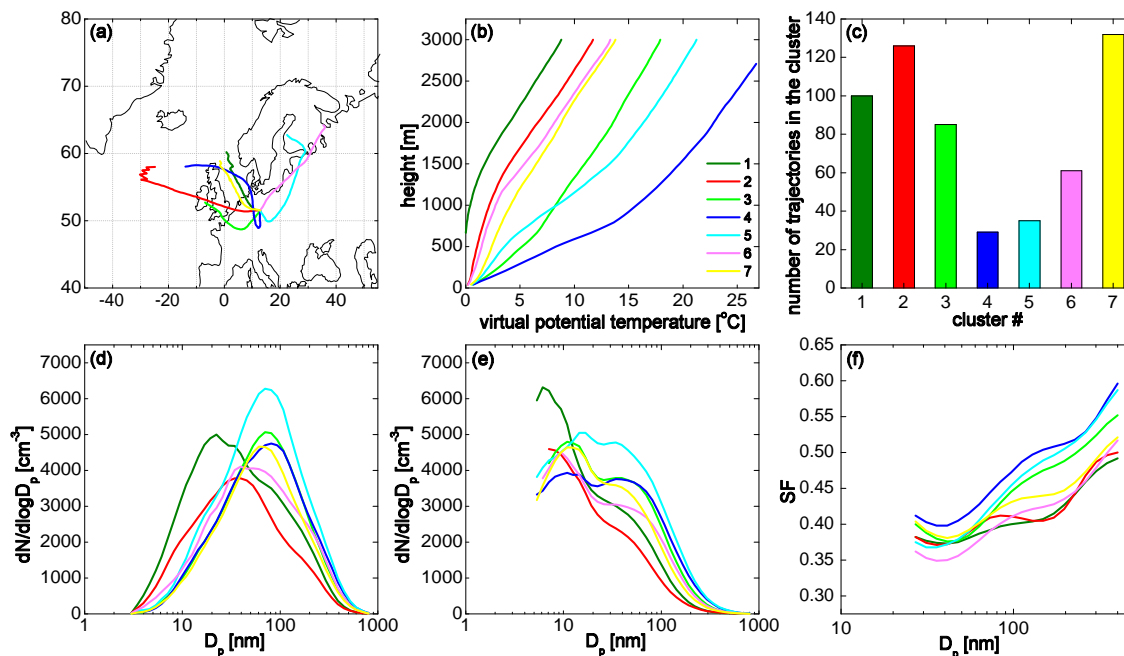


Fig. 8. Back trajectory cluster analysis for 7 air mass types: **(a)** back trajectories, **(b)** vertical profiles of virtual potential temperature, **(c)** number of trajectories in the respective cluster, each corresponding to a time period of 12 h, **(d)** particle size distributions, **(e)** non-volatile size distributions, **(f)** diameter shrinking factors SF.

[Title Page](#)[Abstract](#)[Introduction](#)[Conclusions](#)[References](#)[Tables](#)[Figures](#)[◀](#)[▶](#)[◀](#)[▶](#)[Back](#)[Close](#)[Full Screen / Esc](#)[Printer-friendly Version](#)[Interactive Discussion](#)

Size distributions of non-volatile particle residuals and relation to air mass origin

C. Engler et al.

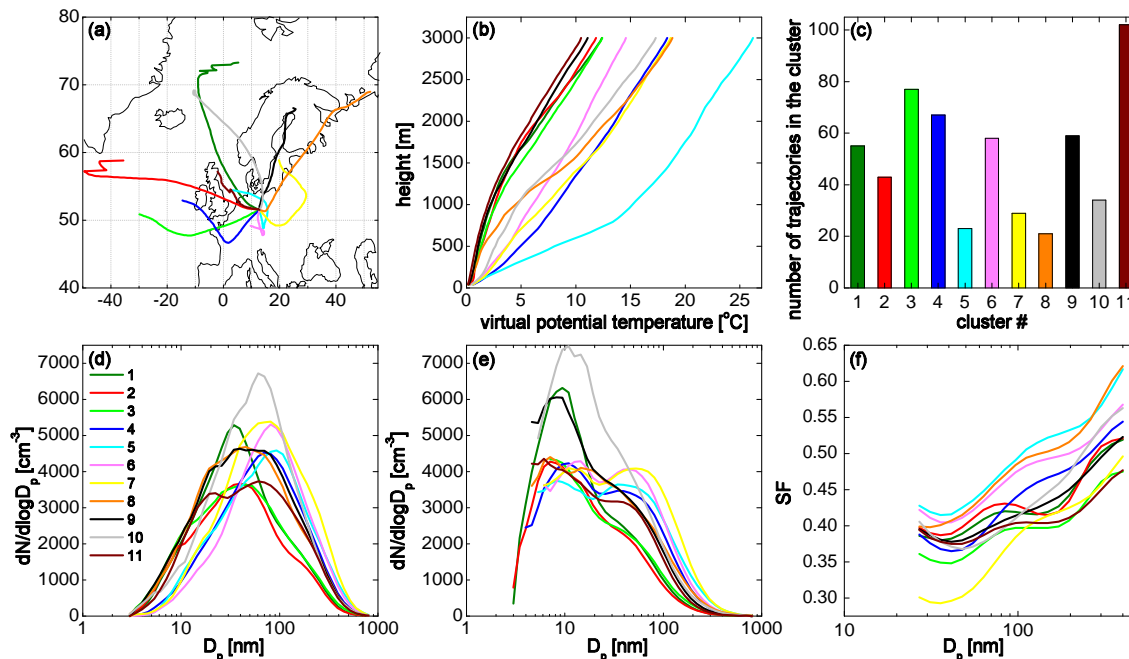


Fig. 9. Back trajectory cluster analysis for 11 air mass types: **(a)** back trajectories, **(b)** vertical profiles of virtual potential temperature, **(c)** number of trajectories in the respective cluster, each corresponding to a time period of 12 h, **(d)** particle size distributions, **(e)** non-volatile size distributions, **(f)** diameter shrinking factors SF.

[Title Page](#)[Abstract](#)[Introduction](#)[Conclusions](#)[References](#)[Tables](#)[Figures](#)[⏪](#)[⏩](#)[⏴](#)[⏵](#)[Back](#)[Close](#)[Full Screen / Esc](#)[Printer-friendly Version](#)[Interactive Discussion](#)